# Effect of path length on valve tray columns : experimental study.

Rim Brahem, Aude Royon-Lebeaud, Dominique Legendre

# Effect of length path on valve tray columns: experimental study

Rim BRAHEM[a], Aude ROYON-LEBEAUD[a], Dominique LEGENDRE[b]

[a] IFP Energies nouvelles, Rond-point de l'échangeur de Solaize, BP 3, 69360 Solaize, France

[b] Institut de Mécanique des Fluides de Toulouse (IMFT), 2 Allée du Professeur Camille Soula, 31400 Toulouse, France

## Abstract

Experimental measurements of hydrodynamic and interfacial area parameters are carried out over two rectangular pilot scale valve tray columns. The effect of tray path length on extrapolation between the two columns is studied and phenomenological correlations for hydrodynamic and interfacial area are proposed. Correlations are compared both to literature and to industrial results showing good agreement and a significant improvement for the prediction of industrial conditions. Discrepancies preventing an accurate description of industrial trends are highlighted through comparison between typical emulsion height profiles on both columns.

***Key words:*** valve trays hydrodynamics, interfacial area, absorption columns, scale up, path length

# 1 Introduction

Natural gas commercialisation is subject to constraining environmental and operational specifications. Such specifications require treatment of gas stream in order to remove several components like water, heavier hydrocarbons, acid gases ($CO_2$, $H_2S$, organic sulphur compounds, COS, $CS_2$, HCN), nitrogen oxides (NOx), sulphur dioxide ($SO_2$), nitrogen compounds, volatile organic compounds (VOCs), volatile chlorine compounds (HCl, $Cl_2$ …) or volatile fluorine compounds (HF, $SiF_4$ …) (Kohl & Nielsen, 1997). Depending on initial gas composition and required product specifications, gas stream is processed through several units (dehydration, desulphurisation, acid gas removal …). For the acid gas removal unit, different kinds of technologies are employed: physical or chemical absorption, physical or chemical adsorption, permeation, redox or cryogenics. Technology choice is mainly based on concentration of acid compounds, partial pressures, selectivity to a specific compound and specifications of final products. Though, the most spread technology is gas liquid absorption using amines solutions.

Valve trays are widely used as contactors for absorption columns because of their relatively low cost and their better performance for specific situations. Within the gas sweetening process context,

mass transfer and hydrodynamics having important effects on column effectiveness and operability, absorption columns design depends greatly on the well determination of hydrodynamics and mass transfer parameters related to gas liquid contactors. Actually this design relies on empirical correlations established on pilot scale units. However existence of considerable discrepancy between sets of correlations encountered in literature makes optimisation of column design difficult to achieve. Experimental works have been carried out on hydrodynamics and mass transfer mainly on sieve trays, and little on valve trays (Zuiderweg & Harmens, 1958; Mc Allister et al., 1958; Barker & Self, 1962 ; Kister & Haas, 1988 ; Colwell, 1981 ; Zuiderweg, 1982 ; Bennett, Agrawal & Cook, 1983 ; Scheffe, 1984 ; Fasesan, 1987 ; Poherecki & Moniuk, 1988 ; Peytavy et al., 1990 ; Liang et al. 2008...). Still malfunctions on industrial columns are related (Kister, 2003 ; Kister & Olsson, 2011) even for sieve trays which have been more frequently studied. Divergences between literature correlations could be attributed to the great number of influent parameters (geometric, operational and physicochemical). Impacts of considerable number of these influent parameters have not been studied thoroughly.

For a given system and an established operational condition, overall hydrodynamic parameters on tray related to absorption effectiveness are mainly clear liquid height $h_{Lc}$, emulsion height $h_{Fe}$ and mean liquid fraction $\alpha_L$. These parameters are related to each other through the following expression:

$$h_L = \alpha_L h_{Fe} \tag{1}$$

Correlations for these three parameters reported in literature can be sorted into two groups regarding the phenomenological description adopted for the gas liquid emulsion flow.

The most used description is the one established on the hypothesis of a homogeneous mixture. This postulate justifies the use of Francis equation describing the height over an exit weir of a stationary fluid flow. When considering the gas-liquid emulsion rate in the Francis equation, correlations for the clear liquid height over the tray are proposed in experimental studies under the following form (Stichlmair, 1978; Hofhuis, 1980 ; Colwell, 1981 ; Bennett et al., 1983 ; El Azrak, 1988 ; Liang et al., 2008 …):

$$h_{Lc} = \alpha_L h_{Fe} = \alpha_L h_w + C\left(\frac{\alpha_L L^2}{g}\right)^{1/3} \tag{2}$$

*L* is the liquid loading defined as

$$L = \frac{Q_L}{L_w} \tag{3}$$

where $Q_L$ is the liquid rate, $L_w$ and $h_W$ are the width and the height of exit weir respectively, *g is the* gravity acceleration and *C* is a constant taking into account the friction on the tray.

The second phenomenological description used for the gas liquid flow is the trajectory model. In this model the liquid progress toward tray exit is the effect of droplets projection over the exit weir. Such description points out the importance of momentum transfer from the ascending gas to the cross liquid flow. As a consequence the flow parameter *FP* representing the ratio between the liquid and the gas inertia is used for correlations describing hydrodynamic parameters:

$$FP = \sqrt{\frac{\rho_L}{\rho_G}} \frac{U_L}{U_G} \tag{4}$$

where $U_L$ is the horizontal liquid velocity defined as

$$U_L = \frac{Q_L}{h_{LC} \times L_w} \tag{5}$$

$U_G$ is the vertical gas velocity toward the active area $A_a$ defined as

$$U_L = \frac{Q_G}{A_a} \tag{6}$$

and $\rho_L$ and $\rho_G$ are the liquid and gas densities, respectively. To access the horizontal liquid velocity $U_L$, the knowledge of clear liquid height $h_{Lc}$ is required. Thus for empirical correlations, different authors have used the flow ratio $\Psi$ instead of the flow parameter *FP* (Dhulesia, 1983 and 1984 ; Békássy-Molnár & Mustafa, 1991 and 1997 …):

$$\psi = FP \times h_{Lc} = \sqrt{\frac{\rho_L}{\rho_G}} \frac{L}{U_G} \tag{7}$$

The clear liquid height is then written as a power law of $\Psi$:

$$h_{Lc} = A \psi^{\alpha} \tag{8}$$

For the mean liquid fraction $\alpha_L$ several studies agree well with the fact $\alpha_L$ is mainly dependent on gas inertia (Bennett et al., 1983; Liang et al., 2008 …). Some efforts have been made to propose dimensional consistent correlations by using the Froude number *Fr,* comparing gas inertia to liquid weight on the tray (Hofhuis, 1980; Colwell, 1981; Zuiderweg, 1982 ; Chen & Fan, 1995):

$$Fr = \sqrt{\frac{\rho_G U_G^2}{g \rho_L h_{Lc}}} \tag{9}$$

The interfacial area and the mass transfer coefficients in both liquid and gas sides are also important parameters for column design. For these parameters less phenomenological descriptions can be found and the reported expressions are mainly put under a power law form (Badssi et al., 1988; Peytavy et al., 1990 ; Pohorecki & Moniuk, 1988…). Furthermore little works on the mass transfer parameters have been made on a reasonably large pilot units to account for the hydrodynamic effects (Scheffe, 1984; El Azrak, 1988 ; Liang et al., 2008). For these parameters the choice of a characteristic liquid velocity seems more problematic as well. Indeed, depending on the considered

study two characteristic liquid velocities are encountered: the liquid loading *L* or the liquid velocity $U_{La}$ toward the active area *Aa*:

$$U_{La} = \frac{Q_L}{A_a} \qquad (10)$$

The effect of column dimensions which impact scalability to larger sizes has been less studied. Studying hydrodynamics on sieve trays, Hofhuis (1980) used two different size columns and proposed dimensional coherent correlations for hydrodynamic parameters and regime transitions. Other works have used different sets of experimental data and have indirectly considered the effect of the column size (Colwell, 1981; Zuiderweg, 1982; Bennett et al, 1983; Chen and Fan, 1995).

Krishna et al. (2003) have carried out a CFD study where the effect of column diameter has been investigated through the modelling of two different columns. In this work the authors showed an important impact of scale effects especially on the mixing characteristics.

In this work the effect of path length $L_P$, the distance travelled by the liquid on a tray between the entrance and the exit weir, is investigated by carrying out hydrodynamic and interfacial area measurements. Two different path lengths are considered: $L_P$=0.36m and $L_P$=0.96m. In literature this geometric parameter has not been studied thoroughly. Table 1 shows some examples of characteristic path lengths $L_P$ from literature. As shown in the table, some works have been conducted on relatively small path lengths $L_P$ in comparison with industrial units.

***Table 1: Examples of $L_P$ (m) values in literature versus industrial units***

| Piqueur & Verhoeye, 1976 | Bennett et al., 1983 | Mustafa & Békássy-Molnár, 1997 | Fasesan, 1987 | Uys et al., 2012 | Liang et al., 2008 | H. Dhulesia, 1984 | Industrial units |
|---|---|---|---|---|---|---|---|
| 0.15 | 0.15 | 0.28 | 0.43 | 0.475 | 0.53 | 0.89 | 0.5/0.8 |

The two columns considered in this work are presented in section 2. Section 3 is dedicated to the comparison of hydrodynamic and interfacial area measurements. In section 4, some attempts are made in order to propose phenomenological and dimensionally coherent correlations for clear liquid height $h_{Lc}$, mean emulsion height $h_{Fe,}$ mean liquid fraction $\alpha_L$ and interfacial area per net area *a'*. The proposed correlations are compared to correlations from the literature in section 5. Section 6 discusses the application of the proposed correlation to industrial cases and present some future works.

# 2 Experimental set up

The present experimental study has been realized on two rectangular pilot columns, C2 and C3, having the same geometrical characteristics but a different path lengths $L_P$ (See figure 1.a). The total tray pressure drop ($\Delta P_{Tray}$) and the emulsion pressure drop ($\Delta P_{Emulsion}$) were measured using Rosemount manometers (see figure 1). $\Delta P_{Emulsion}$ was measured at four different positions and a mean value was considered. Assuming that $\Delta P_{Emulsion}$ is mainly generated by the liquid weight over the tray, the clear liquid height $h_{Lc}$ was evaluated as:

$$h_{Lc} = \frac{\Delta P_{Emulsion}}{\rho_L g} \qquad (11)$$

The emulsion height measurements were made using video records post-processing. For each video a mean emulsion profile is processed and a mean emulsion height $h_{Fe}$ over the tray is measured. More details on hydrodynamic measurements and image processing can be found in Brahem et al., 2013a.

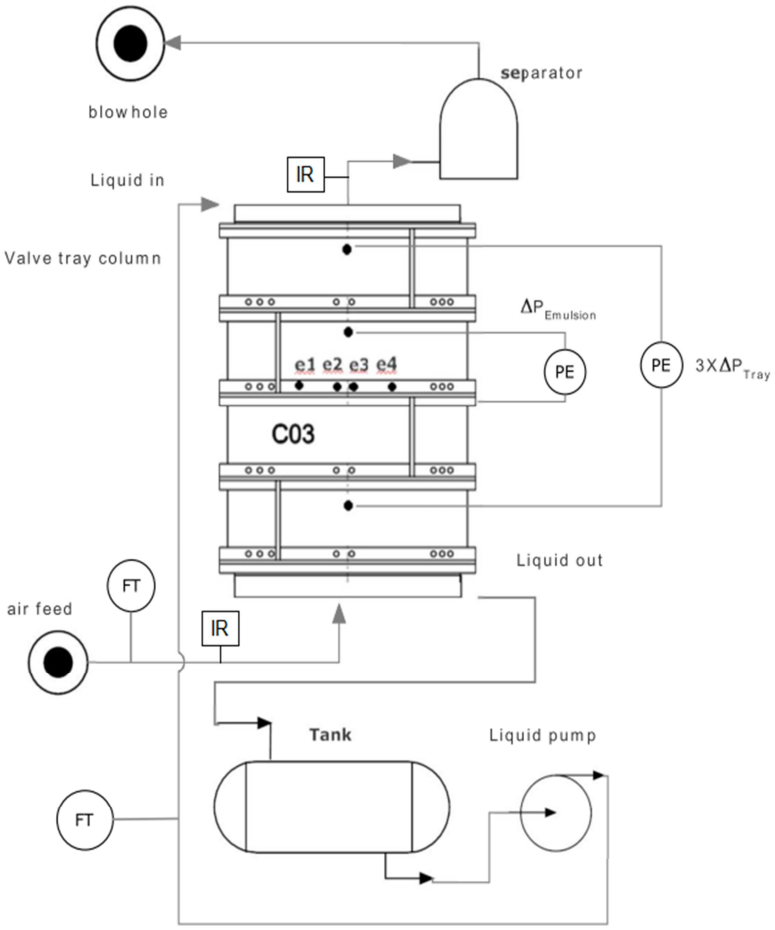


a

| Tray characteristics | | |
|---|---|---|
| | Column C2 | Column C3 |
| Total length (m) | 0,66 | 1,26 |
| Path length $L_P$(m) | 0.36 | 0.96 |
| Total cross section area AT(m²) | 0,13 | 0,24 |
| Active area $A_a$ (m²) | 0,07 | 0,18 |
| Perforated area $A_h$(m²) | 0,011 | 0,032 |
| Weir height $h_w$(m) | 0,065 | |
| Weir length $L_w$(m) | 0,1905 | |
| Plates/ column | 4 | |
| Valves characteristics | | |
| Type | V4R GLITSCH | |
| Valves / tray | 9 | 27 |
| Minimum lift (m) | 0.001 | |
| Maximum lift (m) | 0.009 | |
| Valve diameter (m) | 0.0475 | |
| Hole diameter (m) | 0.039 | |
| valves / m² of active area | 122 | |

b

**Figure 1 : a. Sketch of the experimental set up with the pressure drop connections. b. Geometrical parameters of the two columns C2 and C3**

The interfacial area was measured using an indirect reactive absorption method. The reaction of $CO_2$ absorbed in an aqueous ammonia solution is employed (400ppm $CO_2$ in air/ 0.1N NaOH in water). This method has been validated for interfacial area measurements of structured packing by Alix et al (2011). The absorption reaction can be described by the following set of equilibriums:

$$CO_{2(g)} \leftrightarrow CO_{2(l)}$$

$$CO_{2(l)} + OH^- \leftrightarrow HCO_3^- \qquad (12)$$

$$HCO_3^- + OH^- \leftrightarrow CO_3^{2-} + H_2O$$

The 1st reaction represents the physical absorption of $CO_2$ at the interface. Equilibrium is assumed and represented by the Henry's law:

$$C_{CO_2}^{L,i} = \frac{P_{CO_2}^{G,i}}{He} \qquad (13)$$

The 3rd reaction rate is assumed to be much higher than the 2nd reaction rate (Pinsent et al., 1956, Pohorecki & Moniuk, 1988). Thus the overall kinetic rate is controlled by the 2nd reaction (Pohorecki & Moniuk, 1988):

$$r = k_2 C_{OH^-} C_{CO_2} \qquad (14)$$

In the present study the hydroxide concentration is largely higher than the $CO_2$ concentration, so that the reaction can be considered as pseudo 1st order:

$$r = k_2 C_{OH^-}^0 C_{CO_2} = k' C_{CO_2} \qquad (15)$$

The double film absorption model is considered. The mass transfer from gas to liquid is considered to take place into two thin layers located on both sides of the interface. Assuming equilibrium at the interface and neglecting the resistance to the mass transfer on the gas side ( $P_{CO_2}^{G,i} \approx P_{CO_2}^{G,b}$ ), the $CO_2$ absorbed flux is controlled by the mass transfer processes in the liquid film and by the absorption rate in the liquid:

$$\phi = a \cdot E \cdot k_L \left( C_{CO_2}^{L,i} - C_{CO_2}^{L,b} \right) = a \cdot E \cdot k_L \left( \frac{P_{CO_2}^{G,i}}{He} - C_{CO_2}^{L,b} \right) \qquad (16)$$

where $\Phi$ is the $CO_2$ absorbed flux, $a$ the interfacial area, $E$ the enhancement factor taking into account the contribution of the reaction, $k_L$ the liquid side mass transfer coefficient, $C_{CO_2}^{L,i}$ the $CO_2$ concentration in the liquid at the liquid/gas interface, $C_{CO_2}^{L,b}$ the $CO_2$ concentration in the liquid bulk and $He$ the interfacial equilibrium constant (Henry's law). The enhancement factor depends on 3 parameters:

- The Hatta number *Ha :*

$$Ha = \frac{\sqrt{D_L k_2 C_{OH^-}^0}}{k_L} \quad (17)$$

- The instantaneous enhancement factor, also known as a concentration-diffusion factor

$$E_i = \frac{C_{OH^-}^0}{C_{CO_2}^i} \frac{D_L^{OH^-}}{D_L^{CO_2}} \quad (18)$$

- The ratio between the liquid volume per interfacial area and the liquid film thickness

$$Z_D = \frac{\alpha_L}{a} \frac{k_L}{D_L^{CO_2}} \quad (19)$$

In the case of a fast reaction for which *Ha*>3 and $Z_D$>>1, the enhancement factor can be approximated by the Hatta number $E \approx Ha$ and the $CO_2$ concentration in the liquid bulk is $C_{CO_2}^{L,b} \approx 0$. Consequently the absorbed flux is written as:

$$\phi = a \cdot \sqrt{D_L k_2 C_{OH^-}^0} \left( \frac{P_{CO_2}^{G,b}}{He} \right) \quad (20)$$

Knowing the diffusion constant $D_L$, the Henry's constant *He* and the kinetic constant $k_2$ (constants taken from Pohoericki & Moniuk 1988), the measurement of the $CO_2$ absorbed flux, the $CO_2$ pressure in the gas bulk and the hydroxide concentration allow an indirect determination of the interfacial area

$$a = \frac{\phi}{\sqrt{D_L k_2 C_{OH^-}^0} \left( \frac{P_{CO_2}^{G,b}}{He} \right)} \quad (21)$$

A perfectly agitated flow for the liquid phase and a plug flow for the gas phase are also assumed for the determination of the interfacial area. Two infrared analysers were used at the column entry and exit to measure the $CO_2$ concentrations. The hydroxide concentration in the liquid was measured by titration with HCl.

# 3 Comparison between the two columns

The difference observed between correlations from literature is partially due to the use of different liquid and gas velocities in the experiments. For the liquid velocity two parameters are commonly used, either $U_{La}$ the liquid velocity toward active area (Badssi et al., 1988 ; Scheffe, 1984) or *L* the liquid rate per weir length (or liquid loading) (El-Azrak, 1988 ; Colwell, 1981). The liquid loading divided by the clear liquid height can be considered as a horizontal characteristic liquid velocity in opposition to $U_{La}$ which represents a vertical characteristic velocity.

For the gas velocity, the kinetic factor (the squared root of gas inertia) is usually employed. We consider here two different gas kinetic factors. The first one uses the gas velocity toward the active area $A_a$ while the second one considers the gas velocity toward the net area $A_n = A_a + A_d$ where $A_d$ is the area of one downcomer. The gas kinetic factor toward $A_a$ is

$$Fa = \sqrt{\rho_G U_{Ga}^2} \tag{22}$$

with

$$U_{Ga} = \frac{Q_G}{A_a} \tag{23}$$

The gas kinetic factor toward $A_n$ is

$$Fa = \sqrt{\rho_G U_{Gn}^2} \tag{24}$$

with

$$U_{Gn} = \frac{Q_L}{A_n} \tag{25}$$

In order to identify a pertinent characteristic liquid velocity allowing the comparison between the two columns, the results for the pressure drop, the liquid fraction, the emulsion height and the interfacial area are examined either fixing the liquid velocity toward active area $U_{La}$ or the liquid loading $L$. Corresponding plot for the total pressure drop and the mean emulsion height toward gas kinetic factor $Fa$ are first presented in Figure 2. The Comparison between these two plots seems to indicate that the liquid loading $L$ is more adapted for extrapolation from the little column to the larger one.

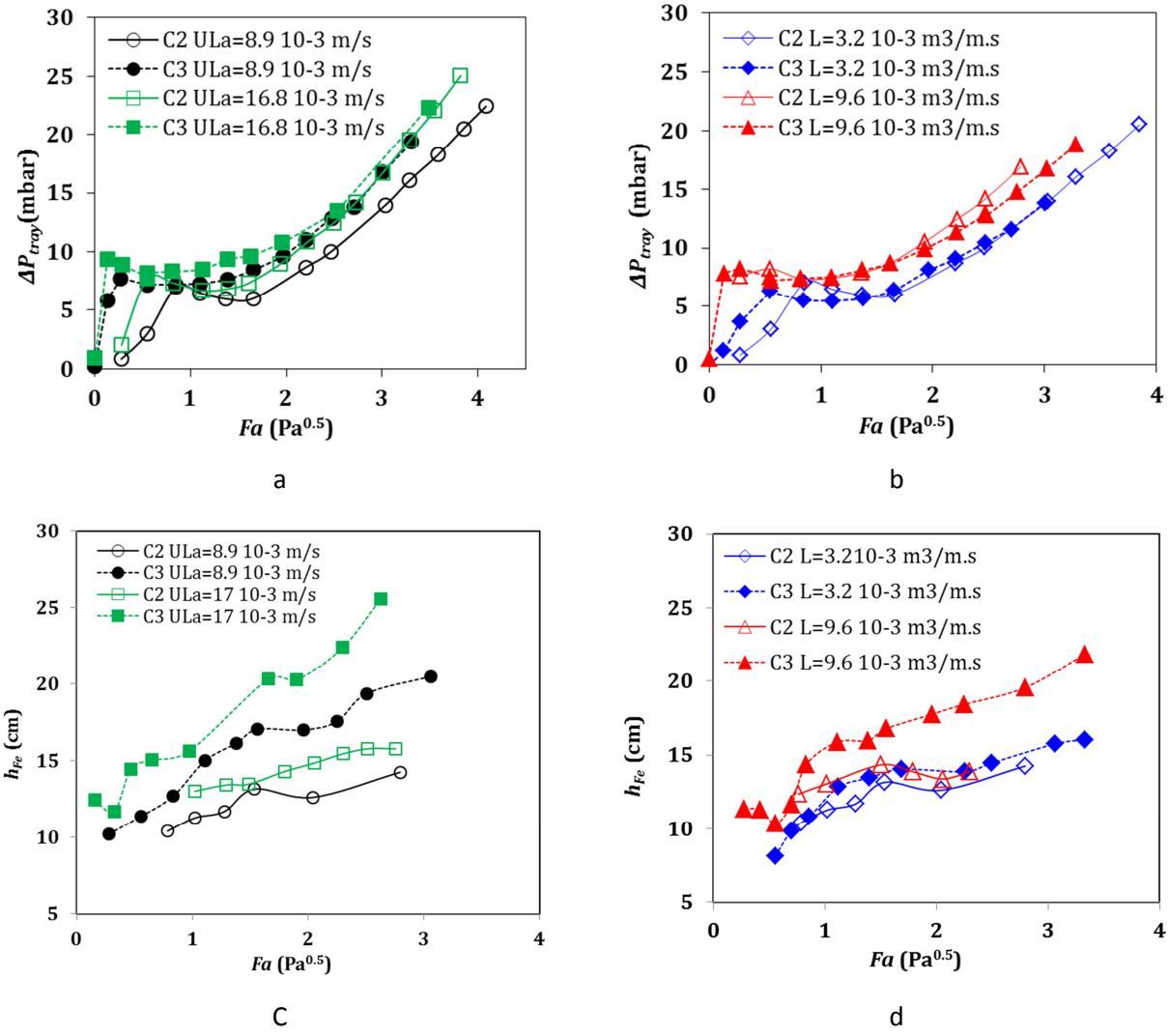


**Figure 2: Comparison of tray pressure drop (a and b) and mean emulsion height (c and d) at a fixed $U_{La}$ (a and c) or at a fixed *L* (b and d)**

Concerning gas velocity, the tray pressure drop is presented in Figure 3 and the mean liquid fraction is shown in Figure 4 for different liquid loading *L* either for a fixed kinetic factor toward the active area *Fa* or for a fixed kinetic factor toward the net area *Fn.* The results suggest that *Fa* is better suited for the comparison of the selected hydrodynamic parameters (pressure drop, emulsion height, mean liquid fraction) especially for intermediate and high velocities. However considering the interfacial area, the choice of *Fn* appears to be more pertinent as shown in Figure 5. This could be explained by the fact that the liquid-gas emulsion is not totally disengaged in the downcomer so that the mass transfer also takes place in the downcomer.

As it may be noticed trough the different plots of the present results for the considered gas and liquid velocities, the choice of a characteristic velocity is made difficult by the little sensitivity of the

measured parameters to these velocities. In some configurations both proposed velocities can be representative: for instance for pressure drop at low gas and liquid rates any velocity could be considered for extrapolation (Figure 2 (a & b) & Figure 3). In some other conditions such as for mean emulsion heights (Figure 1 c & d), the two characteristic velocities fail to superimpose the results for the two columns for moderate to high liquid loads. Such failure to find a similar evolution suggests that the hydrodynamic behaviour between the two columns is not totally identical. In particular, a sharp increase of the interfacial area is noticed when increasing the gas flow rate for the two columns but a different critical value is found (see Brahem et al. 2013, Brahem, 2013 for a detailed description of the hydrodynamic regimes). The limit associated to the increase of interfacial area is related to flooding and lies outside the nominal operating conditions of industrial columns and thus it is of little interest.

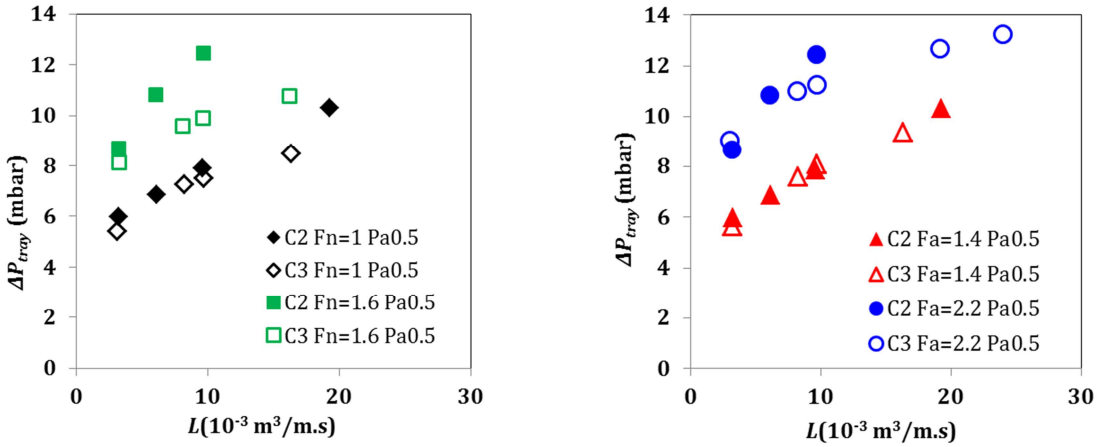


**Figure 3: Comparison of tray pressure drop results. a) At a fixed *Fn* . b) At a fixed *Fa***

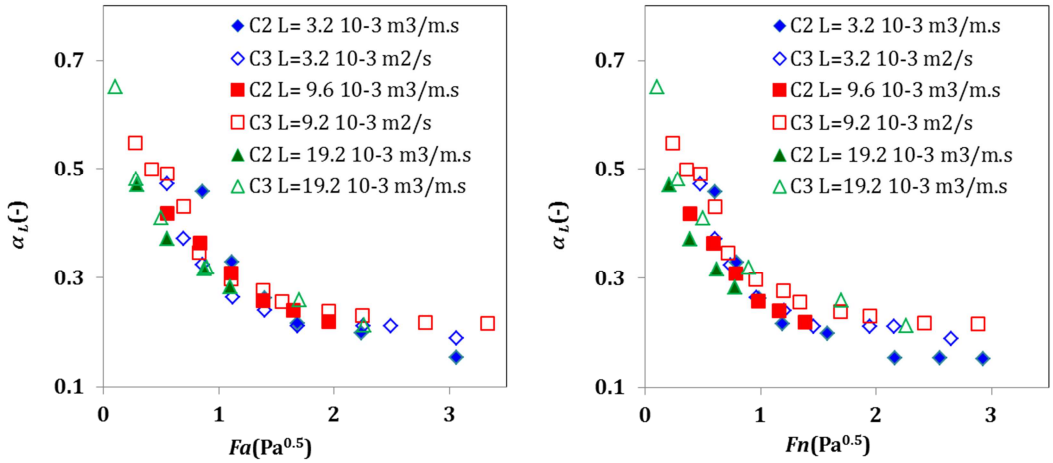


**Figure 4: Mean liquid fraction for two different liquid loadings as a function of gas kinetic factor *Fa***

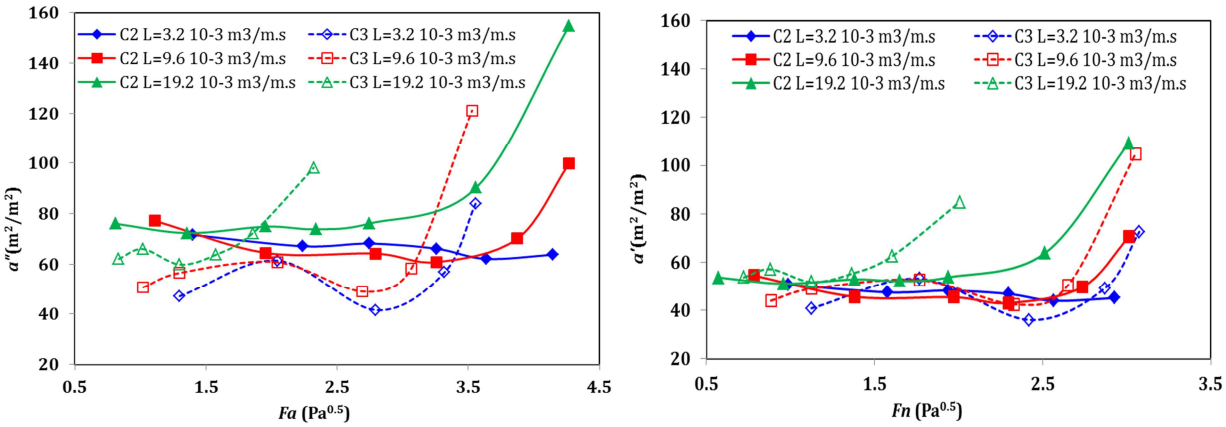


a b

**Figure 5: Interfacial area. a) as a function of *Fa*, b) as a function of *Fn***

Though the similitude between the two columns is not perfect, the observed similarities encourage to consider the scale up and to propose correlations for the emulsion parameters: mean liquid fraction $\alpha_L$, mean emulsion height $h_{Fe}$, mean clear liquid height $h_{Lc}$ and interfacial area per net area *a'*.

# 4 Correlations

In order to propose dimensional homogeneous expressions the choice of adapted parameters is discussed in this paragraph. Once the general form of the correlation is settled, the least square method is used to determine the constant parameters by minimizing the deviation to experimental data.

## *4.1 Mean liquid fraction*

The Froude number has been considered by some authors to describe the evolution of the liquid fraction (Colwell, 1981; Hofhuis, 1980; Chen & Fan, 1995). This choice is also adopted here and the corresponding correlation is expressed as follow:

$$\alpha_L = \frac{1}{1 + a_1 Fr^{\beta_1}} \qquad (26)$$

Such expression has also been suggested in previous studies (Azbel, 1963 ; Kim, 1966 ; Kawagoe et al., 1976 ; Colwell, 1981). From the present experimental results, the values are fixed to $a_1$=11.3 and $\beta_1$=0.54 and the following correlation is proposed:

$$\alpha_L = \frac{1}{1 + 11.3 Fr^{0.54}} \qquad (27)$$

The comparison with experiments is presented in Figure 6 a. For the sake of clarity only results on the larger column C3 are reported in this figure. The parity diagram shown in Figure 6 b corresponds

to the whole set of points obtained for the two columns. The two figures prove that the proposed correlation correctly describes the results obtained for the two columns.

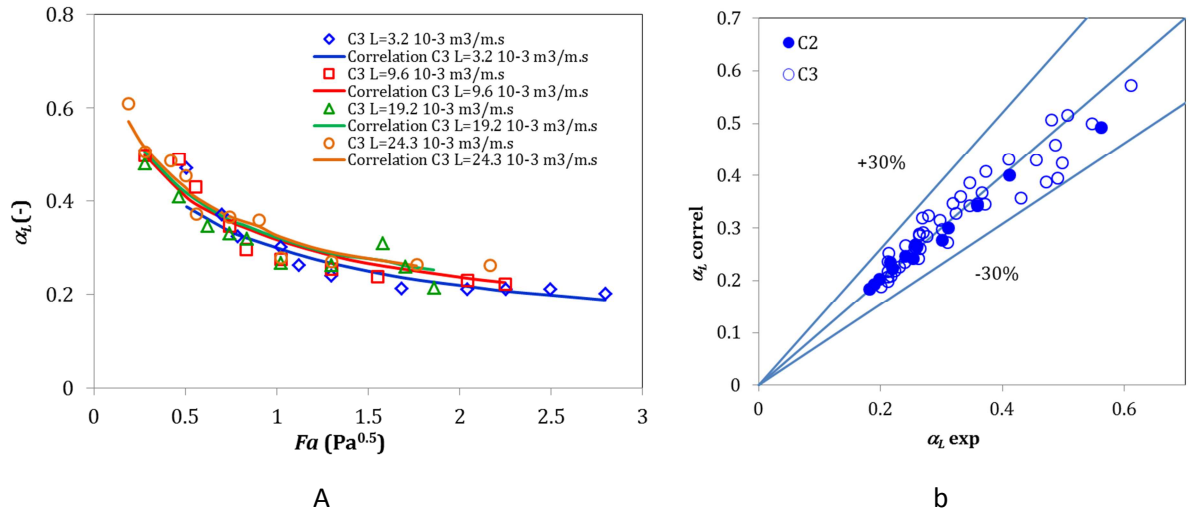


A b

**Figure 6: Liquid fraction. a. Comparison with correlation (27) for the column C3 for different liquid loadings. b. Parity diagram between experiments and correlation (27)**

## *4.2 Clear liquid height*

Several authors have reported that the clear liquid height depends on the hydrodynamic regime (Dhulesia, 1984 ; El-Azrak, 1988 ; Mustafa & Békàssy-Molnar, 1991 & 1997…). Correlations for the clear liquid height for each hydrodynamic regime are proposed by Hofhuis (1980) and Mustapha & Békàssy-Molnar (1997). Hofhuis suggests a transition between the emulsion and the spray regimes for a critical value of the flow parameter *FP* (squared root of liquid to gas inertia) between FP=3 and FP=4. Mustafa & Bekassy (1991) proposed correlations depending on the flow ratio $\Psi$ (=$FP*h_{Lc}$) in which the dependence to this parameter depends on the hydrodynamic regime.

Taking these studies into account, our results for the clear liquid height are represented toward the flow ratio $\Psi$ (see Figure 7). The transition limit is observed for a flow parameter *FP=4* which is coherent with previous studies (Hofhuis, 1980; Zuiderwerg, 1982). For both main hydrodynamic regimes, a correlation for the clear liquid height is determined.

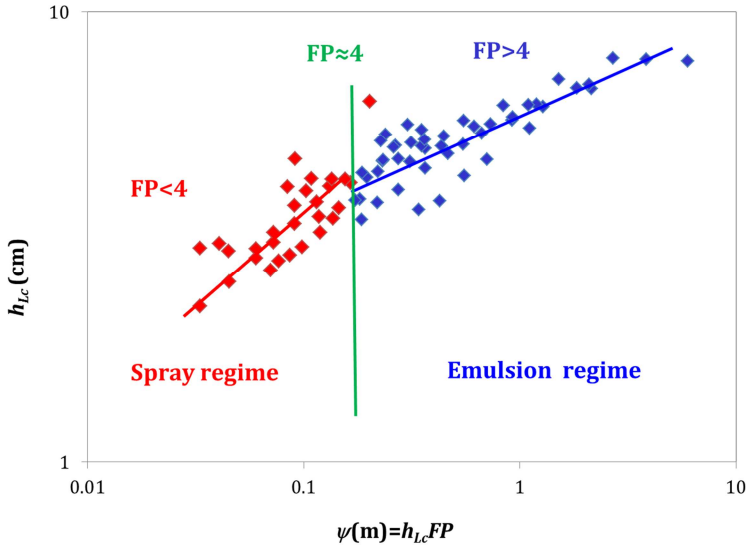


**Figure 7: Identification of the transition between the emulsion and the spray regimes**

Emulsion regime

For the emulsion regime, the two phase flow over the exit weir is commonly described as homogeneous. This description leads to express the clear liquid height under the following form:

$$h_L = \alpha_L h_w + a_2 \left( \frac{\alpha_L L^2}{g} \right)^{1/3} \qquad (28)$$

This form arises from the well-known Francis equation traducing mass conservation of a stationary fluid flow over a weir. Fitting our results in the emulsion regime we found $a_2$=1.315 so that the following correlation is proposed:

$$h_{Lc} = \alpha_L h_w + 1.315 \times \left( \frac{\alpha_L L^2}{g} \right)^{1/3} \qquad (29)$$

## Spray regime

For the spray regime, the trajectory model is usually used to describe the flow on the tray. No explicit form can be easily obtained from this description. In literature (Mustafa & Békassy-Molnar, 1997; Dhulesia, 1984) the flow ratio $\psi$ is commonly used as main correlating parameter. In this work we propose a correlation based on the two main parameters controlling the flow over the tray, namely the flow parameter *FP* and the Froude number *Fr*:

$$h_{Lc} = \frac{\psi}{FP} = \frac{\psi}{a_3 Fr^{\beta_2}} \qquad (30)$$

From our experiments we deduced $\alpha_2$=1.315 and $\beta_2$=1.18 and the following correlation is proposed for the spray regime:

$$h_{Lc} = \frac{\psi}{FP} = \frac{\psi}{0.85Fr^{1.18}} \qquad (31)$$

Figure 8 compares the above correlations in both hydrodynamic regimes to the experiments. Good agreement is encountered for the two columns.

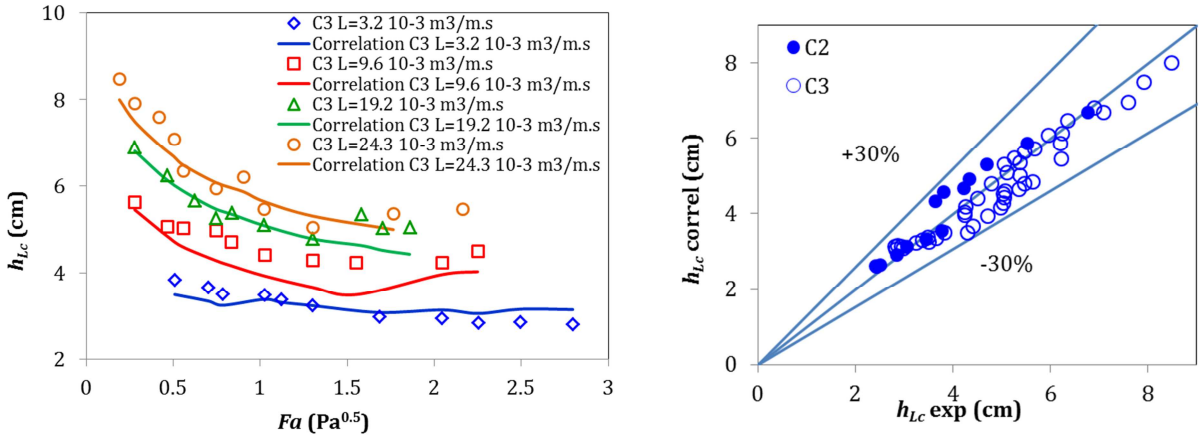


A b

**Figure 8: Clear liquid height. a. Comparison between correlations and experiments for the column C3 for different liquid loadings. b. Parity diagram for the two columns.**

## *4.3 Mean emulsion height*

The evolution of mean emulsion height can now be easily deduced from the mean liquid fraction and the clear liquid height by using relation (1):

$$h_{Fe} = \frac{h_L}{\alpha_L}$$

The corresponding results are reported in Figure 9 where a satisfactory agreement with experimental results is shown. A deviation similar to the one noticed for both mean liquid fraction and clear liquid height is observed.

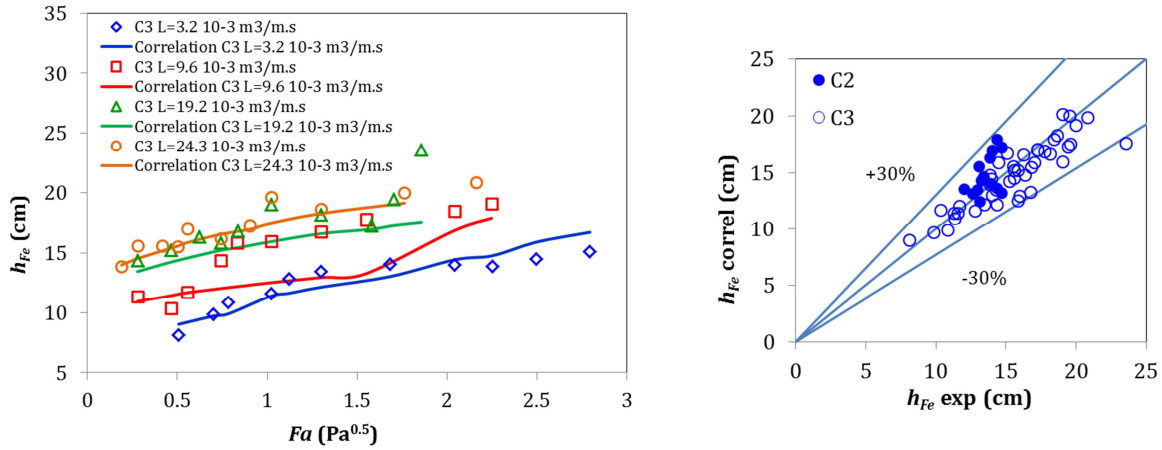


a b

**Figure 9: Mean emulsion height a. Comparison between correlations and experiments for the column C3 for different liquid loadings. b. Parity diagram for the two columns.**

## *4.4 Interfacial area*

In order to propose a dimensionally homogeneous correlation for the interfacial area, we consider the rate of interfacial area. This rate represents the specific interfacial area per unity of emulsion volume. The results obtained for the two columns show that the interfacial area divided by the net area *An* is more adapted for the description of the hole experimental points. To estimate a total emulsion volume, the mean emulsion height is considered. Thus the rate of interfacial area is expressed as follows:

$$a_i = \frac{a}{An \times h_{Fe}} = \frac{a'}{h_{Fe}} \qquad (32)$$

Several works on bubbling flows (Bouaifi et al., 2001; Majumder et al, 2006; Muroyama et al., 2013 …) express this rate of interfacial area as a function of the gas fraction and the maximum bubble size as:

$$a_i = C\frac{\alpha_G}{d_{B\max}} \qquad (33)$$

The maximum bubble size is determined by a critical Weber number $We_{Critical}$ comparing the effect of the surface tension to the inertia that tends to break the interface:

$$We_{Critical} = C'\frac{\rho_L U^2}{\sigma / d_{B\max}} \qquad (34)$$

For the present system of gas injection, we can reasonably consider that the gas inertia controls the bubble size so that we can write:

$$d_{B\max} = C\frac{\sigma}{F_n^2} \qquad (35)$$

The consideration of gas fraction for interfacial rate correlation under a power law form showed no relevant dependency for this reason liquid fraction was considered instead of gas fraction which leads to the final correlation form for interfacial area:

$$a' = \frac{a}{An} = h_{Fe} \times a_4 \frac{F_n^2}{\sigma} \alpha_L^{\beta_3} \qquad (36)$$

From our experiments we obtain $a_4$=6454 and $\beta_3$=4.65 so that the evolution of the interfacial area per net tray area can be described using:

$$a' = 6354 \times h_{Fe} \times \left(\frac{Fn^2}{\sigma}\right) \times \alpha_L^{4.65} \qquad (37)$$

The comparison between this correlation and the experiments is reported in Figure 10. For the larger column C3, the results are quite satisfying, but for the smaller column C2, the correlation underestimates considerably the experimental results. This highlights the fact that the proposed correlation (37) does not reflect the phenomenological mechanism responsible of the production of gas liquid interface. In fact the form proposed is inspired from works done for bubbling regimes while two phase flow on the tray is considerably different because of the gas jets observed near the valves exit and the presence of an emulsion zone above. It is possible that both gas jet dynamics and emulsion behaviour are different between the two columns.

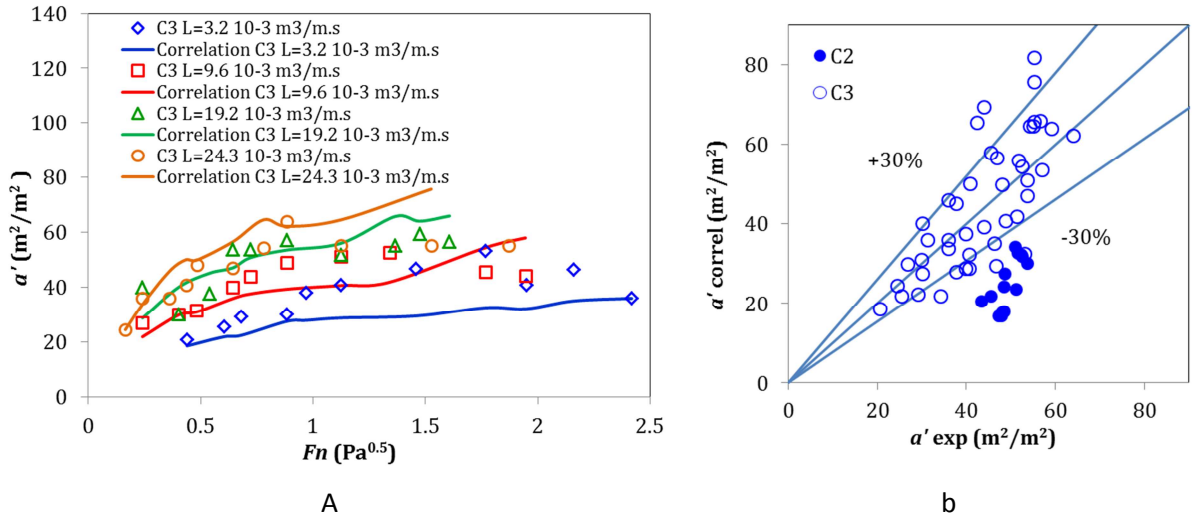


A b

**Figure 10: Interfacial area. a. Comparison between experiments and correlation (37) for column C3 for different liquid loadings. b. Corresponding parity diagram.**

# 5 Comparison to correlations from literature

Several empirical correlations have been proposed in previous works (Dhulesia, 1984 ; El Azrak, 1988 ; Mustafa & Molnár-Bekassy 1997 ; Liang et al, 2008 ; Scheffe, 1984 ; Peytavy et al, 1990). In order to compare these correlations to the relation obtained in our study, we first select some of the most used ones and compare them to our experiments (Figure 11a & Figure 12a). Then we compare our correlations with experimental points issued from other studies (Figure 11b & Figure 12b) for both clear liquid height and interfacial area.

Considering the clear liquid height, the correlations found in literature allow to estimate our experimental results with an error of 60%. The use of our correlation (31) allows reducing the difference on the full data base from the same literature to 40% which is rather satisfactory.

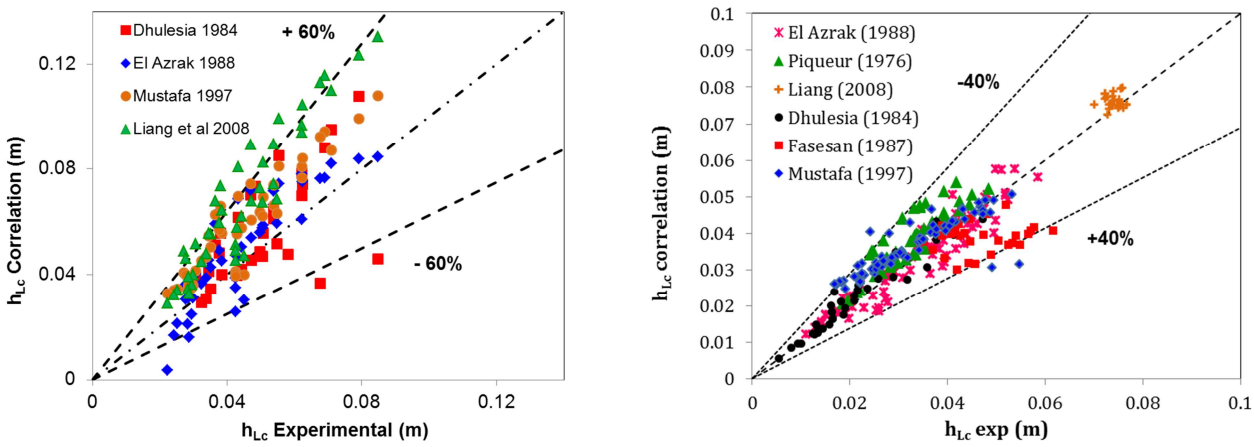


a b

**Figure 11: Clear liquid height a. Correlations from literature compared to present data b. Present correlation (31) applied to literature data**

Considering the interfacial area, the correlations from literature allow to estimate our experiments with an error of 60% while our correlation (37) permits to reduce the error on the full data base of the same literature to 50%. This dispersion is highly dependent on the indirect method used to measure this parameter and the important uncertainties related to the choice of the kinetic and the thermodynamic constants.

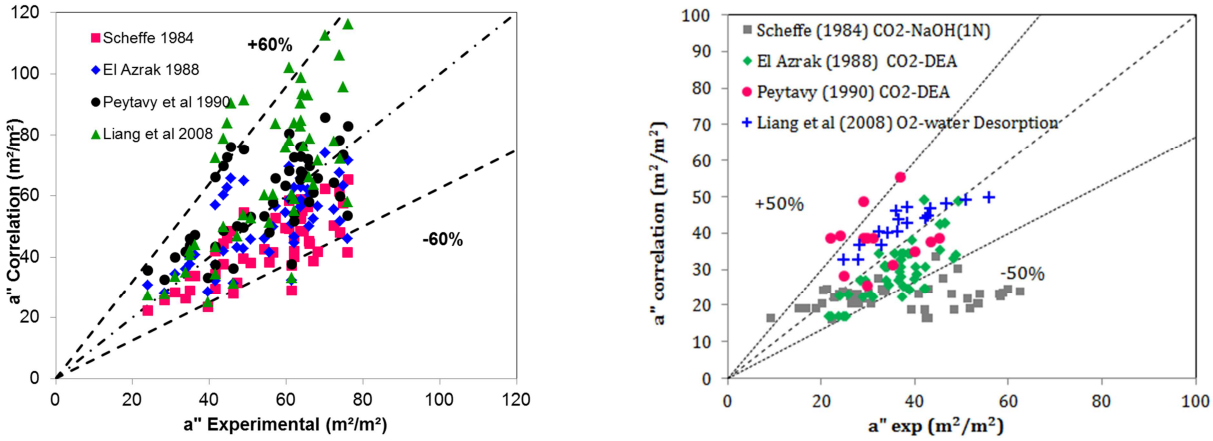


A b

**Figure 12: Interfacial area a. Correlations of literature compared to present data b. Present correlation (37) applied to literature data**

# 6 Application to industrial cases and effect of flow path length

In order to evaluate the accuracy of the correlation for the interfacial area, and in particular its extrapolability, some expressions from literature (El-Azrak, 1988 ; Scheffe, 1984 ; Liang et al, 2008) and from present work are compared to experimental points acquired on industrial columns. The corresponding comparison is presented in Figure 13.

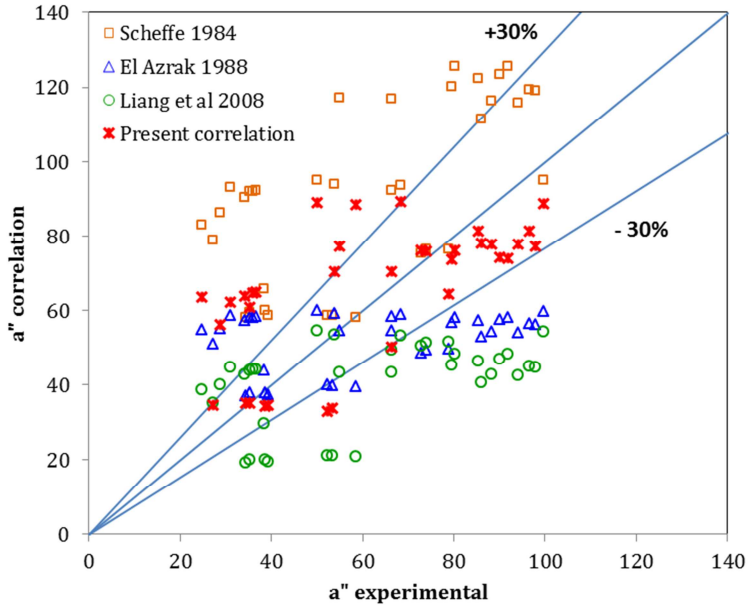


**Figure 13: interfacial area from industrial columns compared to correlation (37) and correlations from literature.**

Figure 13 clearly shows that the proposed correlation allows significantly decreasing the dispersion toward industrial points in comparison with previous expressions. However none of the correlations

including the relations proposed in this study succeeds in properly describing the trend of the experimental points. Differences between predicted values and experimental points are clearly not due to some experimental error measurements, indicating that some important phenomena are not considered in the proposed models.

A scale effect has been noticed when comparing results between the two columns. A perfect similitude can not be shown even when considering different liquid and gas velocities.

Figure 14 reports the clear liquid height and the mean emulsion height for the two columns.

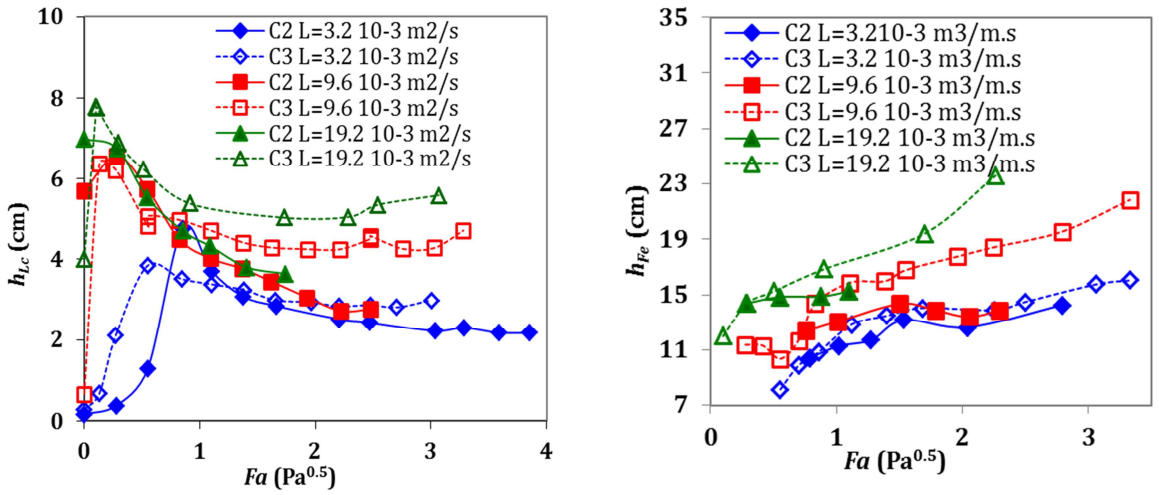


a b

**Figure 14 : Comparison between the two columns for different liquid loads *L* and toward gas kinetic factor *Fa*. a. Clear liquid height $h_{Lc}$ b. Mean emulsion height $h_{Fe}$**

In Figure 14 a similar behaviour for $h_{Lc}$ is noticeable with two recognisable zones when the gas velocity increases. The first zone corresponding to the increase of $h_{Lc}$ is characterised by an important amount of weeping. In the second zone, increasing the gas velocity results in a drop of the clear liquid height (Brahem et al 2013). The differences lie in a lower dependence to the liquid load on the smaller column C2 and a higher dependence to the gas kinetic factor especially for the second zone. Figure 14 b reports the mean emulsion height. The results for the smaller column show a small dependence with both gas and liquid velocities. Comparable values for the larger column C3 are only observable at low gas kinetic factors.

To better understand these discrepancies, typical emulsion profiles are compared between the two columns in Figure 15. Considering the large column, it is shown that for a fixed liquid loading and an increasing gas kinetic factor four different behaviors can be identified (Brahem et al 2013a) while for the small column only three behaviors are observed (Brahem et al 2013b). For the low gas velocities a dumping regime with a highly oscillating profile but rather homogeneous along the tray is noticed for both columns. When increasing the gas velocity for C3 a channeling regime followed by a homogeneous regime are observed while for the column C2 only a regime with a bell-shaped

emulsion profile is noticed. Approaching flooding (high gas velocities) a channeling phenomenon is noticed for C3 while profiles for C2 are transformed into a more parabolic form. Moreover the profiles for C2 are less dependent to the gas and the liquid flow rates. As shown in Figure 15.b and Figure 15.c**,** the profiles for the two columns seem to be similar at both the entrance and the exit of the tray. This is due to the fact the profile is fully controlled by the border conditions imposed on the tray extremities. However, at the middle of the tray, the emulsion profiles do differ between the two columns. For the larger column, the path length $L_P$ is large enough for the profile to become stable and independent from the border conditions. However for the small column $L_P$ is rather short and the profile is totally controlled by border conditions. This could provide the explanation for the lower dependence of emulsion height to gas and liquid velocities observed in the column C2.

These observations highlight an intrinsic scale effect on hydrodynamic behavior of the two phases flow. Such change in behavior between small and large columns could help to explain the differences noticed between proposed correlations and industrial results.

In addition to geometric scaling effects (dead zone for example), the effects of physicochemical properties and their dependence to operating conditions (pressure and temperature) as well as to the gas and liquid compositions have not been investigated through this work. They are expected to influence hydrodynamic and mass transfer behaviours and could also be at the origin of the differences noticed between proposed correlations and industrial results.

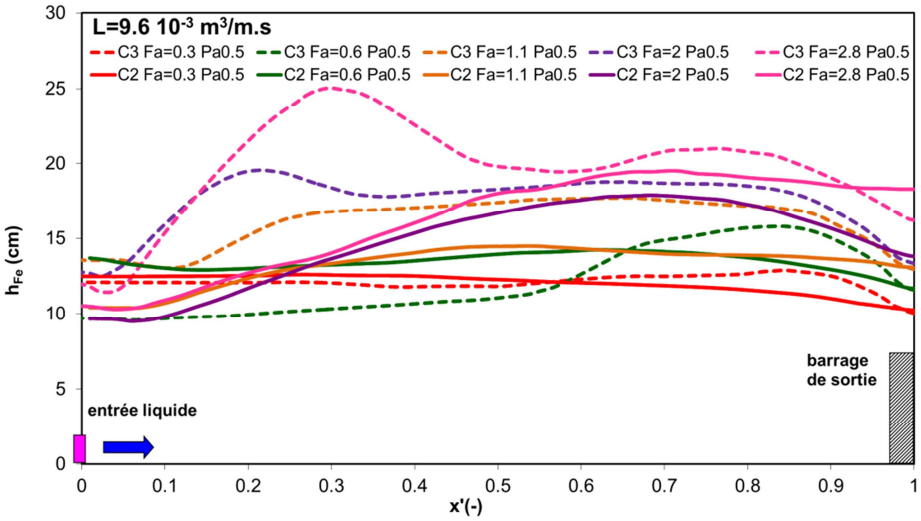


a

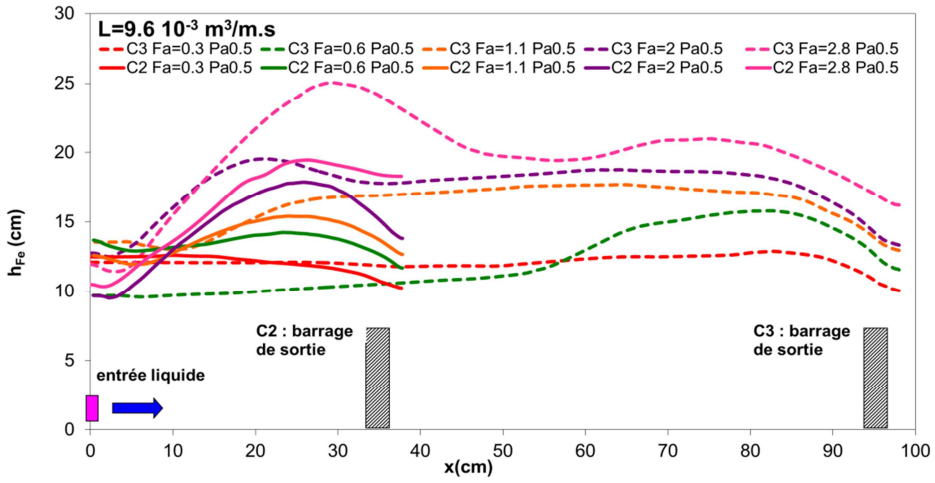


b

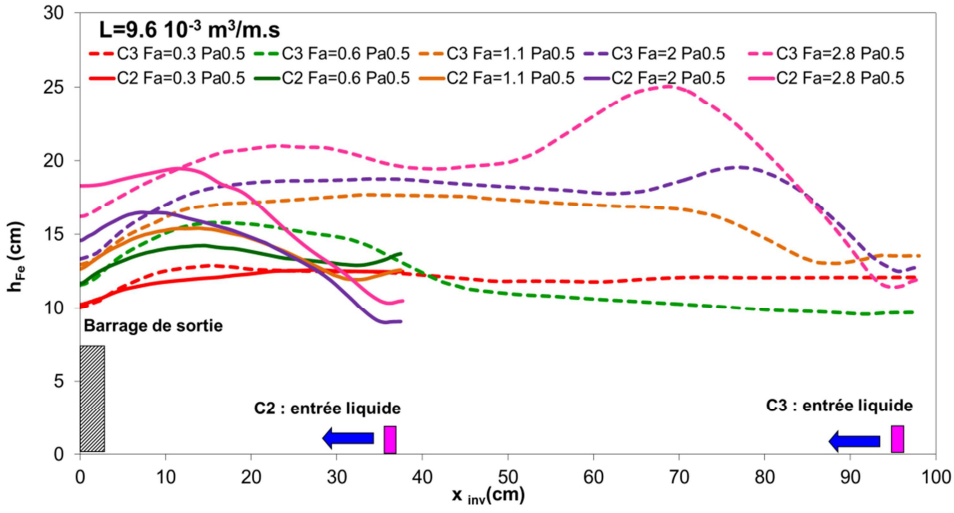


c

**Figure 15: Emulsion profiles for the two columns. a) As a function of the distance from the liquid entry normalised by the path length *Lp*. b) As a function of the distance from the liquid entry. c) As a function of the distance from the exit weir.**

# 7 Conclusions

Experiments have been carried out on two different path length columns to provide a wide data base for hydrodynamic parameters and interfacial area on valve trays. Correlations for liquid fraction, clear liquid and emulsion heights and interfacial area have been proposed based on phenomenological descriptions. These correlations allow representing present experimental data with a maximum error of 40% for hydrodynamic parameters and 50% for interfacial area for the two columns considered. Moreover the proposed correlation for the interfacial area improves representativeness for available data from both literature and industrial tests compared to previous correlations (Liang et al 2008, Scheffe 1984 and El Azrak 1988).

However the new relation proposed for the description of the interfacial area fails to take into account the scale effect because of a non-negligible impact of the boundary conditions for the small path length column. This dependence due to the impact of the border conditions leads to different emulsion profiles and different regime transitions between the two columns. Moreover other parameters of influence such as physicochemical parameters have not been considered. Their effect is expected to be important and thus has to be quantified in the future.

# 8 Nomenclature

| | | |
|---|---|---|
| $A_a$ | $m^2$ | Active or bubbling area |
| $A_h$ | $m^2$ | Perforated area |
| $A_T$ | $m^2$ | Total column cross area |
| $d_h$ | m | Hole diameter |
| $d_V$ | m | Valve diameter |
| $Fa$ | $Pa^{0.5}$ | Kinetic gas factor based on velocity toward active area |
| $G$ | $m.s^{-2}$ | Gravity acceleration |
| $h_{Fe}$ | m | Emulsion height on the tray |
| $h_{Lc}$ | m | Clear liquid height on the tray |
| $h_w$ | m | Exit weir height |
| $L$ | $m^3.m..s^{-1}$ | Liquid loading or liquid flow rate per unit weir length |
| $L_D$ | m | Downcomer length |
| $L_P$ | m | Length flow path |
| $L_T$ | m | Total column length |
| $L_w$ | m | Exit weir length |
| $P$ | Pa | Pressure |
| $Q_G$ | $m^3.s^{-1}$ | Gas flow rate |
| $Q_L$ | $m^3.s^{-1}$ | Liquid flow rate |
| $T_s$ | m | Tray spacing |
| $U_{G,a}$ | $m.s^{-1}$ | Gas velocity toward active area |
| $U_{G,h}$ | $m.s^{-1}$ | Gas velocity toward perforated area |
| $U_L$ | $m.s^{-1}$ | Liquid velocity defined in relation (5) |
| $U_{L,a}$ | $m.s^{-1}$ | Liquid velocity toward active area |
| ***Dimensionless numbers*** | | |
| $C_D$ | - | Friction coefficient |
| $FP'$ | - | Flow parameter, represents the square root of the ratio between liquid inertia and gas inertia |
| $Fr$ | - | Froude number opposing gas inertia toward active area to liquid weight on the tray |
| $Fr_h$ | - | Froude number using gas velocity toward perforated area |
| ***Greek letters*** | | |
| $\alpha_L$ | - | Mean liquid hold up on tray |
| $\Delta P_{Dry}$ | Pa | Valves (or tray) pressure drop measured in absence on liquid flow |
| $\Delta P_{Emulsion}$ | Pa | Pressure drop due to emulsion on tray |
| $\Delta P_{Tray}$ | Pa | Tray pressure drop |
| $\Delta P_{Valves}$ | Pa | Valves pressure drop measured in presence on liquid flow |
| $\mu_{G/L}$ | Pa.s | Gas/liquid viscosity |
| $\rho_G$ | $kg.m^{-3}$ | Gas density |
| $\rho_L$ | $kg.m^{-3}$ | Liquid density |
| $\Psi$ | m | Flow ratio opposing liquid loading time square root liquid density and kinetic gas factor |

# 9 Bibiliography


Alix, P., Raynal, L., Meyer, M., Prevost, M., & Rouzineau, D. (2011). Mass transfer and hydrodynamic characteristics of new carbon carbon packing : Application to CO 2 post-combustion. *Chemical Engineering Research and Design*, *89*(May), 1658–1668. doi:10.1016/j.cherd.2010.09.023

Azbel, D. S. (1963). The hydrodynamics of bubbler processes. *Int. Chem. Engng*, *3*(3), 319.

Badssi, A., Bugarel, R., Blanc, C., Peytavy, J. L., & Laurent, A. (1988). Influence of Pressure on the Gas-Liquid Interfacial Area and the Gas-side Mass Transfer Coefficient of a Laboratory Column Equipped with Cross-Flow Sieve Trays. *Chem. Eng. Process.*, *23*, 89–97.

Barker, P. E., & Self, M. F. (1962). The evaluation of liquid mixing effects on a sieve plate using unsteady and steady state tracer techniques. *Chemical Engineering Science*, *17*(7), 541–554. doi:10.1016/0009-2509(62)87005-5

Békássy-Molnár, E., & Mustafa, H. (1991). Clear liquid height on sieve plates in the froth, mixed and spray regimes. *Trans IChemE*, *69*, 14–20.

Bennett, D. L., Agrawal, R., & Cook, P. J. (1983). New pressure drop correlation for sieve tray distillation columns. *AIChE Journal*, *29*(3), 434–442. doi:10.1002/aic.690290313

Bouaifi, M., Hebrard, G., Bastoul, D., & Roustan, M. (2001). A comparative study of gas hold-up, bubble size, interfacial area and mass transfer coefficients in stirred gas–liquid reactors and bubble columns. *Chemical Engineering and Processing: Process Intensification*, *40*(2), 97–111. doi:http://dx.doi.org/10.1016/S0255-2701(00)00129-X

Brahem, R., Royon-Lebeaud, A., Legendre, D., Moreaud, M., & Duval, L. (2013). Experimental hydrodynamic study of valve trays. *Chemical Engineering Science*. doi:10.1016/j.ces.2013.03.030

Chen, G. X., & Fan, Z. (1995). *Models for liquid head, pressure drop and weeping* (p. 33).

Colwell, C. J. (1981). Clear height and froth density on sieve trays. *Ind. Eng. Chem. Process Des. Dev.*, *Vol. 20*(2), p 298–307.

Dhulesia, H. (1984). Clear liquid height on sieve and valve trays. *Chemical engineering research & design*, *62*(5), 321–326.

Dhulesia, H. A. (1983). Operating flow regimes on the valve tray. *Chemical Engineering Research and Design*, *Volume 61a*, 329 – 332.

El Azrak, A. (1988). *Etude des plateaux à clapets caractérisation du transfert de matière et de l'hydrodynamique*. Institut National Polytechnique de Toulouse.

Fasesan, S. (1987). Hydraulic characteristics of sieve and valve trays. *Industrial & engineering chemistry research*, *26*(10), 2114–2121.

Hofhuis, P. A. . (1980). *Flow regimes on sieve trays for gas/liquid contacting*. TECHNISCHE HOGESCHOOL DELFT.

Kawagoe, K., Nakado, T., & Otake, T. (1976). Flow pattern and gas hold up conditions in gas sparged contactors. *Int. Chem. Engng*, *16*(1), 176.

Kim, S. K. (1966). Theoretical study of vapour-liquid hold up on a perforated plate. *Int. Chem. Engng*, *6*(4), 634.

Kister, H Z. (2003). WHAT CAUSED TOWER MALFUNCTIONS IN THE LAST 50 YEARS ?, *81*(January).

Kister, H. Z., & Haas, J. R. (1988). Entrainment from Sieve Trays in the Froth Regime. *Ind. Engi. Chem. Res.*, *27*, 2331–2341.

Kister, H. Z., & Olsson, M. (2011). Understanding maldistribution in 3-pass trays. *Chemical Engineering Research and Design*, *89*(8), 1397–1404. doi:10.1016/j.cherd.2011.01.030

Liang, Y., Zhou, Z., Shao, M., Geng, J., Wu, Y., & Zhang, Z. (2008). The Impact of Valve Tray Geometry on the Interfacial Area of Mass Transfer, *54*(6). doi:10.1002/aic

Liang, Y., Zhou, Z., Shao, M., Geng, J. (2008). The impact of valve tray geometry on the interfacial area of mass transfer. *AIChE Journal*, *54*(6), pp.1470–1477.

Majumder, S. K., Kundu, G., & Mukherjee, D. (2006). Bubble size distribution and gas–liquid interfacial area in a modified downflow bubble column. *Chemical Engineering Journal*, *122*(1–2), 1–10. doi:http://dx.doi.org/10.1016/j.cej.2006.04.007

Mc Allister, R. A., McGinnis, J. P. H., & Plank, C. A. (1958). Perforated -plate performance. *Chemical Engineering Science*, *9*.

Muroyama, K., Imai, K., Oka, Y., & Hayashi, J. (2013). Mass transfer properties in a bubble column associated with micro-bubble dispersions. *Chemical Engineering Science*, *100*(0), 464–473. doi:http://dx.doi.org/10.1016/j.ces.2013.03.043

Mustafa, H., & Békássy-Molnár, E. (1997). Hydrodynamic Characteristics of Nutter Valve Trays, New Correlations. *Chemical Engineering Research and Design*, *75*(6), 620–624. doi:10.1205/026387697524146

Peytavy, J. L., Huor, M. H., Bugarel, R., & Laurent, A. (1990). Interfacial Area and Gas-Side Mass Transfer Coefficient of a Gas-Liquid Absorption Column : Pilot-Scale Comparison of Various Tray Types. *Chem. Eng. Process.*, *27*, 155–163.

Piqueur, H., & Verhoeye, L. (1976). RESEARCH ON VALVE TRAYS. HYDRAULIC PERFORMANCE IN THE AIR-WATER SYSTEM. *Canadian Journal of Chemical Engineering*, *54*(3), (pp.177–184.

Pohorecki, R., & Moniuk, W. (1988). Plate Efficiency in the Process of Absorption with Chemical Reaction - Experiments and Example Calculations. *The Chemical Engineering Journal*, *39*, 37–46.

Scheffe, R. D. (1984). Mass transfer characteristics of valve trays. (PhD thesis, Clarkson University, Potsdam, NY, USA)

Stichlmair, J. (1978). Dimensionierung des Gas/Flüssigkeit-Kontaktapparates Bodenkolonne, Teil 2. Chemie Ingenieur Technik, 50(5), 383-387.

Uys, E. C., Schwarz, C. E., Burger, A. J., & Knoetze, J. H. (2012). New froth behaviour observations and comparison of experimental sieve tray entrainment data with existing correlations. *Chemical Engineering Research and Design*, *90*(12), 2072–2085. doi:10.1016/j.cherd.2012.05.008

Zuiderweg, F. J. (1982). Sieve trays : A view on the state of the art. *Chemical Engineering Science*, *10*, 1441–1464.

Zuiderweg, F. J., & Harmens, A. (1958). The influence of surface phenomena on the performance of distillation. *ChemicalEngineering Science Génie Chimique*, *9*.